Zygmunt PIATEK[1], Bernard BARON[2], Paweł JABŁOŃSKI[1], Tomasz SZCZEGIELNIAK[1], Dariusz KUSIAK[1], Artur PASIERBEK[2]

Czestochowa University of Technology (1), The Silesian University of Technology (2)

A numerical method for current density determination in three-phase bus-bars of rectangular cross section

Abstract. *This paper presents a new numerical computation method for determining the current distributions in high-current three-phase busducts of rectangular busbars. This method is based on the integral equation method and the Partial Element Equivalent Circuit (PEEC) method. It takes into account the skin effect and proximity effects, as well as the complete electromagnetic coupling between phase bars and the neutral bar. In particular, the current densities in rectangular busbars of unshielded three-phase systems with rectangular phase and neutral busbars, and the use of the method are described. Finally, two applications to three-phase unshielded systems busbars are presented.*

Streszczenie. *W artykule przedstawiono nową numeryczna metodę obliczania rozkładu gęstości prądu w szynoprzewodach prostokątnych trójfazowego toru wielkoprądowego. Metoda wykorzystuje równie całkowe i oparta jest na teorii obwodowych cząstkowych elementów zastępczych. Uwzględnia ona zjawisko naskórkowości i zbliżenia oraz całkowite sprzężenie magnetyczne miedzy szynoprzewodami fazowymi i szynoprzewodem neutralnym. W szczególności opisano rozkład gęstości prądu i zastosowanie tej metody dla przypadku trójfazowego toru wielkoprądowego o prostokątnych szynoprzewodach fazowych i prostokątnym szynoprzewodzie neutralnym. Rozkłady gęstości prądów wyznaczono dla dwóch przykładów układów trójfazowych z szynoprzewodami prostokątnymi.(**Numeryczna metoda obliczania gęstości prądu w trójfazowym układzie szynoprzewodów prostokątnych.**)*

Keywords: Rectangular busbar, high-current bus duct, current density, numerical method.
Słowa kluczowe: Prostokątny przewód szynowy, tor wielkoprądowy, gęstość prądu, metoda numeryczna.

Introduction

High-current air-insulated bus duct systems with rectangular busbars are often used in power generation and substation, due to their easy installation and utilization. The increasing power level of these plants requires an increase in the current-carrying capacity of the distribution lines (usually 1-10 kA). The medium voltage level of the generator terminals is 10-30 kV. The construction of busbar is usually carried out by putting together several flat rectangular bars in parallel for each phase in order to reduce thermal stresses. The spacing between the bars is made equal to their thickness for practical reasons, and this leads to skin and proximity effects. The bus ducts usually consist of aluminum or copper busbars [1, 2]. A typical cross-section of the unshielded three-phase high-current bus duct is depicted in Fig. 1.

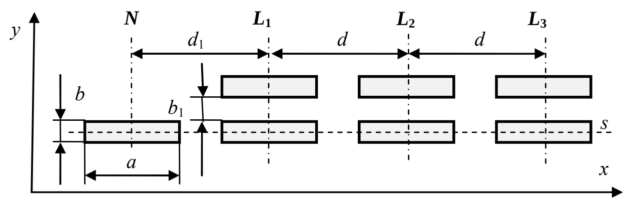

Fig. 1. Three phase high-current bus duct of rectangular cross-section with two busbars per phase and one neutral busbar

The distribution of AC current density in the cross-section of each busbar of a system of busbars is generally non-uniform, and known as “skin effect”. It can be found exactly only for simple geometries like round wires and tubes [3-7], or very long and thin rectangular busbars (tapes or strips) [7-10]. For more complex cross-sections, analytical-numerical and numerical methods must be used to find the current distributions, which is further modified by the proximity of other conductors – “proximity effect” [11-17]. Both the skin effect and proximity effect will generally cause the current distribution is not uniform over the cross section of a busbar. Since the current distributions influence the AC inductances and resistances of the busbars, the voltage regulation and power loss of a system is affected by the design of its current busses. The development of efficient numerical methods for the solutions of these problems is therefore of interest.

Integral equation

The integral formulation is well known [3, 4, 18-24] and is derived by assuming sinusoidal steady-state, and then applying the magnetoquasistatic assumption that the displacement current, $\mathrm{j}\omega\varepsilon\underline{\boldsymbol{E}}$, is negligible. In the case of N straight parallel conductors with length l, conductivity σ_i (i = 1, 2,…, N), cross section S_i with sinusoidal current input function with angular frequency ω and complex value $\underline{I}_i$ flowing in the direction of Oz, the complex current density has one component along the Oz axis, that is $\underline{\boldsymbol{J}}_i(X) = \mathbf{a}_z\underline{J}_i(X)$. The component $\underline{J}_i(X)$ is independent of variable z, and in a general case, depends on the self current and on the currents in the neighboring conductors (the skin and proximity effects). Then also the vector magnetic potential $\underline{\boldsymbol{A}}(X) = \mathbf{a}_z\underline{A}(X)$, the electric field $\underline{\boldsymbol{E}}(X) = \mathbf{a}_z\underline{E}(X)$, and the ideal conductor constitutive relation is $\underline{\boldsymbol{J}}_i(X) = \sigma_i\underline{\boldsymbol{E}}_i(X)$. Then, the integral equation for i^{th} conductor is given as follows

$$\frac{\underline{J}_i(X)}{\sigma_i} + \frac{\mathrm{j}\omega\mu_0}{4\pi}\sum_{j=1}^{N}\int_{v_j}\frac{\underline{J}_j(Y)}{\rho_{XY}}\,\mathrm{d}v_j = \underline{u}_i\,, \tag{1}$$

where $X = (x_1, y_1, z_1)$ is the observation point, $Y = (x_2, y_2, z_2)$, is the source point, $\rho_{XY} = |X - Y|$ is the distance between the observation point X and the source point Y (Fig.2), v_i and v_j are the volume of the i^{th} and the j^{th} conductor, respectively, $\underline{u}_i$ is the unit voltage drop (in V·m^{-1}) across the i^{th} conductor, and i, j = 1, 2,…, N.

Then, by simultaneously solving Eq. (1) with the current conservation, $\nabla\cdot\underline{\boldsymbol{J}}(X) = 0$, the conductor current densities and the unit voltage drops can be computed. In the case shown in Fig. 1, the following integral equation can be written for arbitrary point X in each busbar and the enclosure:

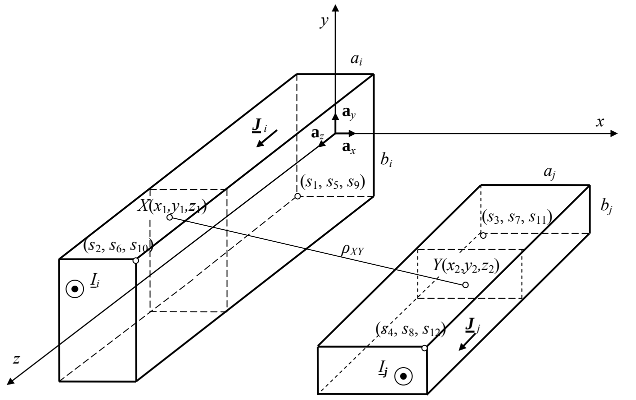

Fig. 2. The i^{th} and j^{th} conductors of a system of N parallel busbars of rectangular cross section

(2) $$\frac{\underline{J}_{i,k}(X)}{\sigma_i}+\frac{\mathrm{j}\omega\mu_0}{4\pi}\sum_{j=1}^{N_c}\sum_{l=1}^{N_j}\int_{v_{t,l}}\frac{\underline{J}_{j,l}(Y)}{\rho_{XY}}\,\mathrm{d}v_{j,l}=\underline{u}_i\,,$$

where:
- N_c is the number of phases plus the neutral plus the enclosure, and i, j = 1, 2,…, N_c (N_c = 5),
- N_j is the number of busbars belonging to one phase or the neutral or the number of rectangular plates of which the enclosure consists (usually 4), and k, l = 1, 2,…, N_j.

Multiconductor model of the busbars

In this model, each phase, neutral busbars and each plate of enclosure is divided in several thin subbars [2, 25-30], as shown in Fig. 3.

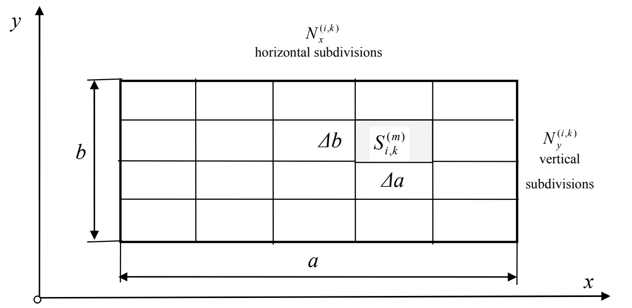

Fig. 3. The k^{th} bar of the i^{th} phase divided into $N_{i,k}=N_x^{(i,k)}N_y^{(i,k)}$ subbars

This division of the k^{th} bar of the i^{th} phase or the neutral into subbars is carried out separately for the horizontal (Ox axis) and vertical (Oy axis) direction of its cross-sectional area. Hence, subbars are generally rectangular in the cross-section, with the width Δa and thickness Δb, defined by the following relations:

(3) $$\Delta a=\frac{a}{N_x^{(i,k)}}\quad\text{and}\quad\Delta b=\frac{b}{N_y^{(i,k)}}\,,$$

where a and b are the width and the thickness of the busbar, respectively, $N_x^{(i,k)}$ and $N_y^{(i,k)}$ are the number of divisions along the busbar width and thickness respectively. Thus, the total number of subbars of the k^{th} bar of the i^{th} phase is $N_{i,k}=N_x^{(i,k)}N_y^{(i,k)}$, and they are numbered by m = 1, 2, …, $N_{i,k}$. For the l^{th} bar of the j^{th} phase or the neutral we have the total number of subbars $N_{j,l}=N_x^{(j,l)}N_y^{(j,l)}$ numbered by n = 1, 2, …, $N_{j,l}$. All subbars have the same length l.

If the area $S_{i,k}^{(m)}=\Delta a\cdot\Delta b$ of the m^{th} subbar is very small and the diagonal $[(\Delta a)^2+(\Delta b)^2]^{1/2}$ of it is not greater than skin depth, we can neglect the skin effect and assume that the complex current density can be considered uniform, i.e.

(4) $$\underline{J}_{i,k}^{(m)}=\frac{\underline{I}_{i,k}^{(m)}}{S_{i,k}^{(m)}}$$

where $\underline{I}_{i,k}^{(m)}$ is the complex current flowing through the m^{th} subbar.

Busbar impedances

For the m^{th} subbar or plate the integral equation (2) can be written as

(5) $$\frac{\underline{J}_{i,k}^{(m)}(X)}{\sigma_i}+\frac{\mathrm{j}\omega\mu_0}{4\pi}\sum_{j=1}^{N_c}\sum_{l=1}^{N_j}\sum_{n=1}^{N_{j,l}}\int_{v_{t,l}}\frac{\underline{J}_{j,l}^{(n)}(Y)}{\rho_{XY}}\,\mathrm{d}v_{j,l}^{(n)}=\underline{u}_i$$

where $v_{j,l}^{(n)}$ is the volume of the n^{th} subbar or plate of the l^{th} bar or plate of the j^{th} phase or the neutral or the enclosure.

Now, we can divide Eq. (5) by the area $S_{i,k}^{(m)}$ and integrate over the volume $v_{i,k}^{(m)}$ of the m^{th} subbar or plate, obtaining the following equation:

(6) $$R_{i,k}^{(m)}\underline{I}_{i,k}^{(m)}+\mathrm{j}\omega\sum_{j=1}^{N_c}\sum_{l=1}^{N_j}\sum_{n=1}^{N_{j,l}}M_{(i,k)(j,l)}^{(m,n)}\underline{I}_{j,l}^{(n)}=\underline{U}_i\,,$$

where $\underline{U}_i$ is the voltage drop across of all subbars of the i^{th} phase or the neutral or the shield (they are connected in parallel), and the resistance of the m^{th} subbar is defined by

(7) $$R_{i,k}^{(m)}=\frac{l}{\sigma_i S_{i,k}^{(m)}}\,,$$

and the self or the mutual inductance is expressed as

(8) $$M_{(i,k)(j,l)}^{(m,n)}=\frac{\mu_0}{4\pi\,S_{i,k}^{(m)}S_{j,l}^{(n)}}\int_{v_{i,k}^{(m)}}\int_{v_{j,l}^{(n)}}\frac{\mathrm{d}v_{i,k}^{(m)}\,\mathrm{d}v_{j,l}^{(n)}}{\rho_{XY}}\,.$$

The exact closed formulae for the self and the mutual inductance of rectangular conductor of any dimensions, including any length, are given in [19] and [20] respectively. Not only do not we use the geometric mean distance here, we do not use the formula for mutual inductance between two filament wires as well.

The set of equations like as (6), written for all subbars, forms the following general system of complex linear algebraic equations

(9) $$\underline{\hat{\boldsymbol{U}}}=\underline{\hat{\boldsymbol{Z}}}\,\underline{\hat{\boldsymbol{I}}}\,,$$

where $\underline{\hat{\boldsymbol{U}}}$ and $\underline{\hat{\boldsymbol{I}}}$ are column vectors of the voltages and currents of all subbars, respectively, and $\underline{\hat{\boldsymbol{Z}}}$ is the symmetric matrix of self and mutual impedances (the impedance matrix) of all subbars, the elements of which are

(10) $$\underline{Z}_{(i,k)(j,l)}^{(m.n)}=\begin{cases}R_{i,k}^{(m)}+\mathrm{j}\omega\,M_{(i,k)(j,l)}^{(m,n)} & m=n, i=j, k=l,\\ \mathrm{j}\omega\,M_{(i,k)(j,l)}^{(m,n)} & \text{otherwise.}\end{cases}$$

Then, we can find the admittance matrix $\underline{\hat{\boldsymbol{Y}}}$, which is the inverse matrix of the impedance matrix $\underline{\hat{\boldsymbol{Z}}}$, and it is expressed as

$$\hat{\mathbf{Y}} = \left[\underline{Y}^{(m,n)}_{(i,k)(j,l)}\right] = \hat{\mathbf{Z}}^{-1}, \tag{11}$$

and has a similar structure as $\hat{\mathbf{Z}}$. Then it is possible to determine the current of the m^{th} subbar of the k^{th} bar of the i^{th} phase or the neutral as

$$\underline{I}^{(m)}_{i,k} = \sum_{j=1}^{N_c}\sum_{l=1}^{N_j}\sum_{n=1}^{N_{j,l}} \underline{Y}^{(m,n)}_{(i,k)(j,l)}\underline{U}_j . \tag{12}$$

The total current of the i^{th} phase or the neutral is

$$\underline{I}_i = \sum_{k=1}^{N_i}\sum_{m=1}^{N_{i,k}} \underline{I}^{(m)}_{i,k} . \tag{13}$$

By inserting Eq. (12) into Eq. (13), we obtain

$$\underline{I}_i = \sum_{j=1}^{N_c} \underline{Y}_{i,j}\underline{U}_j , \tag{14}$$

where

$$\underline{Y}_{i,j} = \sum_{k=1}^{N_i}\sum_{m=1}^{N_{i,k}}\sum_{l=1}^{N_j}\sum_{n=1}^{N_{j,l}} \underline{Y}^{(m,n)}_{(i,k)(j,l)} . \tag{15}$$

From the admittance matrix with elements given by Eq. (15), we can determine the impedance matrix of a shielded three-phase system busbars with the neutral busbar as follows

$$\underline{\mathbf{Z}} = \left[\underline{Z}_{i,j}\right] = \underline{\mathbf{Y}}^{-1} = \left[\underline{Y}_{i,j}\right]^{-1} . \tag{16}$$

Since each $\underline{Z}_{i,j}$ is obtained from a matrix whose elements are comprised of information related only to construction and material, its value is not affected by the busbar current. In spite of that the skin and proximity effects are taken into consideration.

Current densities

If we assume all sinusoidal phase currents to be given, we can write that the neutral current $\underline{I}_N = \underline{I}_1 + \underline{I}_2 + \underline{I}_3$ and, from Eq. (14), find all voltages across phase and neutral busbars as

$$\underline{U}_i = \sum_{j=1}^{N_c} \underline{Z}_{i,j}\underline{I}_j . \tag{17}$$

Thus, from that and Eq. (12) it is possible to determine all currents in subbars, and finally calculate, according to Eq. (4), current densities in them. These densities differ across the cross sections of the busbars due to the skin and proximity effects.

Numerical examples

The first numerical example selected for this paper features a three-phase system of rectangular busbars with one neutral busbar, whose cross-section is depicted in Fig.1. According to the notations applied in this figure, the following geometry of the busbars has been selected: the dimensions of the phase rectangular busbars and the neutral busbars are a = 60 mm, $b = b_1$ = 5 mm, $d = d_1$ = 90 mm. The phase busbars and the neutral are made of copper, which has the electric conductivity of σ = 56 MS·m^{-1}. The frequency is 50 Hz. All phases have two busbars per phase − $N_1 = N_2 = N_3 = 2$, and the neutral has one busbar − $N_4 = 1$. The length of the busbar system is assumed l = 10 m. In the numerical procedure, each phase busbar is divided into $N_x^{(i,k)}$ = 30 and $N_y^{(i,k)}$ = 5, which gives 150 subbars for each busbar. Hence, all three phases and the neutral busbars have 1050 subbars in total. With the chosen division, each rectangular subbar has dimensions of 2 × 1 mm. This allows for the fact that the current density is uniform on the surface of the subbars. During the simulation, three balanced currents with busbar-rated values I_1 = 1 kA are imposed in phases as shown

$$\underline{I}_2 = \underline{I}_1\mathrm{e}^{-\mathrm{j}120^\circ}, \quad \underline{I}_3 = \underline{I}_1\mathrm{e}^{\mathrm{j}120^\circ}, \quad \text{and} \quad \underline{I}_N = \underline{I}_1 + \underline{I}_2 + \underline{I}_3 = 0. \tag{18}$$

As a first result, the current density comparison along x axis, practically the same along y axis at x = const, in each busbar is shown in Fig. 4.

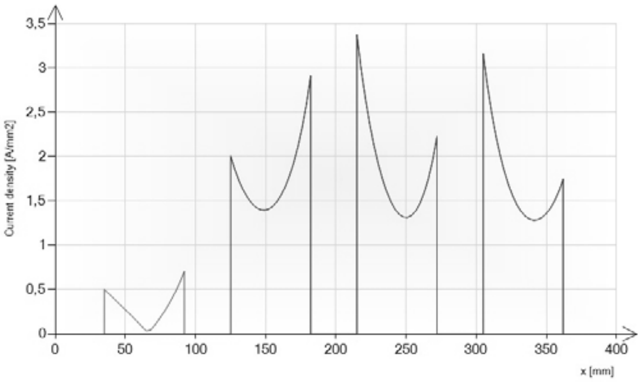

Fig. 4. Current density along line s (see Fig. 1) in busbars of the high-current three-phase busducts with two busbars per phase and one neutral bar in the case of three balanced current

The case of three unbalanced currents

$$\underline{I}_2 = 0.5\underline{I}_1\mathrm{e}^{-\mathrm{j}120^\circ}, \quad \underline{I}_3 = \underline{I}_1\mathrm{e}^{\mathrm{j}120^\circ}, \quad \text{and} \quad \underline{I}_N = \underline{I}_1 + \underline{I}_2 + \underline{I}_3 = 0.5\,\mathrm{e}^{\mathrm{j}60^\circ} \tag{19}$$

has been also investigated – Fig. 5.

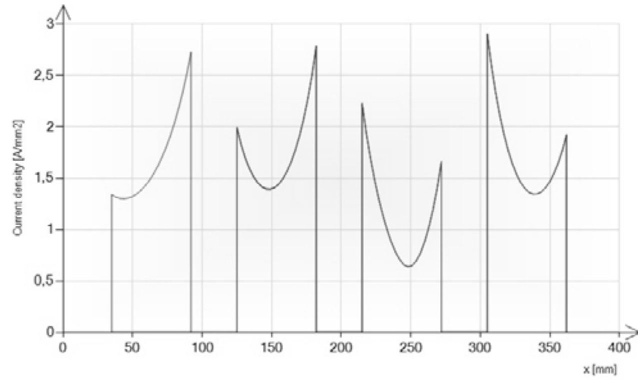

Fig. 5. Current density along line s (see Fig. 1) in busbars of the high-current three-phase busducts with two busbars per phase and one neutral bar in the case of three unbalanced current

The second configuration of a three phase busbar system, the current density of which are investigated, is shown in Fig. 6. It has only one busbar per phase and neutral - $N_1 = N_2 = N_3 = N_4 = 1$. The length of the busbar system and the busbar division are as in the previous example (150 subbars for each busbar). Hence, all three phase and the neutral busbars have 600 total subbars. With the chosen division, each rectangular subbar has still dimensions of 2 × 1 mm. During the simulation, three balanced – Eq. (18) − and three unbalanced – Eq. (19) − currents with busbar-rated values I_{eff} = 1 kA are imposed in phases, and the current densities comparison along x axis, practically the same along y axis at x = const., in each busbar are shown in Fig. 7 and Fig. 8, respectively.

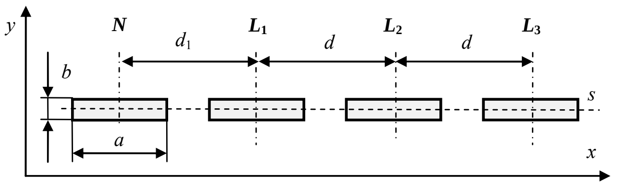

Fig. 6. Three phase high-current bus duct of rectangular cross-section with one busbar per phase and one neutral busbar

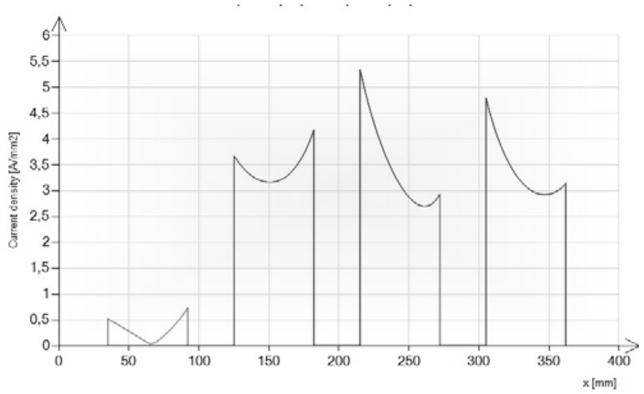

Fig. 7. Current density along line s (see Fig. 6) in busbars of the high-current three-phase busducts with one busbar per phase and one neutral bar in the case of three balanced current

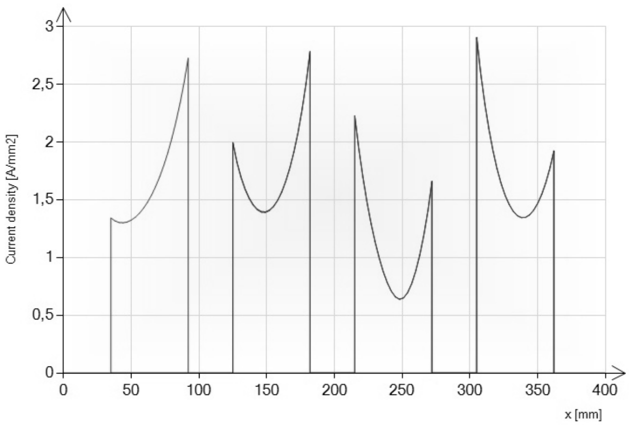

Fig. 8. Current density along line s (see Fig. 6) in busbars of the high-current three-phase busducts with one busbar per phase and one neutral bar in the case of three unbalanced current

Conclusions

A novel approach to the solution of current density distribution in the high-current bus ducts of rectangular cross-section has been presented in this paper. The proposed approached combines the Partial Element Equivalent Circuit (PEEC) method with the exact closed formulae for AC self and mutual inductances of rectangular conductors of any dimensions, which allows the precise accounting for the skin and proximity effects. Complete electromagnetic coupling between the phase busbars and the neutral busbar is taken into account as well.

As Figures 4 and 5 as well as 7 and 8 show, both the skin effect and proximity effect will generally cause the current density in the busbars has a strongly non-uniform distribution across each busbar. Moreover, the distributions are different in individual busbars. Knowing the current distribution is important in evaluating the electrodynamic force on each busbar. It is possible also to evaluate the temperature of the different components of the busbar system.

The proposed method allows us to calculate the current density distribution in a set of parallel rectangular busbars of any constant cross-sections including any length. However, the current density vector is assumed to have only a z-component independent on z, which means that the fringing is neglected, and therefore the length should be large enough. The basic difference between the proposed model and existing models is that it uses expressions for inductances for subbars of finite dimensions. To obtain more accurate results, the fringing must be taken into account, but it requires a 3D model, which is much more time and memory consuming.

The validity of our numerical method has been successfully compared with a classical finite element method (FEM) such a FLUX2D software in the case of 2D busbar systems, particularly for the long busbars.

The proposed model is strikingly simple, and from a logical stand-point can be applied in general to conductors of any constant cross-section, whereas many conventional methods, being much more complicated, often require a greater or lesser degree of symmetry. From the practical stand-point of the calculations involved, the model requires the solution of a rather large set of linear simultaneous equations. However, this solution is well within the range of the ability of existing computers, even those slightly overage.

Acknowledgment

This work was supported by the National Science Centre, Poland, under Grant No. N N511 312540.

REFERENCES

[1] Ducluzaux A.: *Extra losses caused in high current conductors by skin and proximity effects*. Schneider Electric "Cahier Technique" no. 83, 1983.

[2] Sarajčev P. and Goič R.: *Power loss computation in high-current generator bus ducts of rectangular cross-section*. Electris Power Components and Systems, No. 39, 2010, pp. 1469-1485.

[3] Piątek Z.: *Impedances of tubular high current busducts*. Polish Academy of Sciences. Warsaw 2008.

[4] Piatek Z.: *Self and mutual impedances of a finite length gas insulated transmission line (GIL)*. Elec. Pow. Syst. Res., No. 77, 2007, pp. 191-203.

[5] Morgan V.T., Findlay R.D. and Derrah S.: *New formula to calculate the skin effect in isolated tubular conductors at low frequencies.* IEE Proc. Meas. Technol., Vol. 147, No. 4, 2000, pp. 169-171.

[6] Ferkal K., Poloujadoff M. and Dorison E.: *Proximity effect and eddy current losses in insulated cables.* IEEE Trans. on Power Delivery, Vol. 11, No. 3, 1996, pp. 1171-1177.

[7] Kazimierczuk M. K.: *High-frequency magnetic components.* J Wiley & Sons, Chichester, 2009.

[8] Kosek M., Truhlar M. and Richter A.: *Skin effect in massive conductor at technical frequencies.* Przegląd Elektrotechniczny (Electrical Review), R. 87, No. 5, 2011, pp. 179-185.

[9] Kosek M., Truhlar M. and Richter A.: *Skin effect in conductor of rectangular cross-section – approximate solution.* Przegląd Elektrotechniczny (Electrical Review), R. 88, No. 7a, 2012, pp. 23-25.

[10] Abdelbagi H.A.: *Skin and proximity effect in two parallel plates.* Thesis of Master of Science in Engineering, Wirght State University, 2007.

[11] Canova A. and Giaccone L.: *Numerical and analytical modeling of busbar systems.* IEEE Trans. on Power Delivery, vol. 24, No. 3, July 2009, pp. 1568- 1577.

[12] Sigg H.J. and Strutt M.J.O.: *Skin effect and proximity effect in polyphase systems of rectangular conductors calculated on an RC network*. IEEE Trans. on Power Apparatus and Systems, Vol. PAS-89, No. 3, 1970, pp. 470-477.
[13] Dawson F.P, Cao M. and Jain P.K.: *A simplified approach to calculating current distribution in parallel power busses.* IEEE Trans. on Magnetics, Vol. 26, No. 2, 1990, pp. 971-974.
[14] Bourmanne P. et al.: *Skin effect and proximity effect in multiconductor systems with applied currents and voltages.* J. Appl. Phys., Vol. 69, No. 8, 1991, pp. 5035-5037.
[15] Greconici M., Madescu G. and Mot M.: *Skin effect in a free space conductor*. Facta Universitatis (NIŠ), Ser. Elec. Energ., Vol. 23, No. 2, 2010, pp. 207-215.
[16] Jafari-Shapoorabadi R., Konrad A. and Sinlair A.N.: *Comparison of three formulations for eddy-current and skin effect problems.* IEEE Trans. on Magnetics, Vol. 38, No. 2, 2002, pp. 617-620.
[17] Rolicz P.: *Skin effect in a system of two rectangular conductors carrying identical currents.* Electrical Engineering, No. 82, 2000, pp.285-290.
[18] Piątek Z. and Baron B.: *Exact closed form formula for self inductance of conductor of rectangular cross section.* Progress in Electromagnetics Research M. Vol. 26, 2012, pp. 225-236.
[19] Piątek Z. et al: *Exact closed form formula for mutual inductance of conductors of rectangular cross section*. Przegląd Elektrotechniczny (Electrical Review), R. 89, No. 3a, 2013, pp. 61-64.
[20] Piątek Z. et al: *Self inductance of long conductor of rectangular cross section.* Przegląd Elektrotechniczny (Electrical Review), R. 88, No. 8, 2012, pp. 323-326.
[21] Piątek Z. et al: *Mutual inductance of long rectangular conductors.* Przegląd Elektrotechniczny (Electrical Review), R. 88, No. 9a, 2012, pp. 175-177.
[22] Broydé, F., Clavelier E. and Broydé L.: *A direct current per-unit-length inductance matrix computation using modified partial inductance*. Proc. Of the CEM 2012 Int. Symp. on Electromagnetic Compatibility, Rouen, 25-27 April, 2012.
[23] Deeley E. M. and Okon E. E.: *An integral method for computing the inductance and a.c. resistance of parallel conductors*. International Journal for Numerical Methods in Engineering, Vol. 12, 625—634, 1978.
[24] Konrad A.: *Interodifferential finite element formulation of two-dimensional steady-state skin effect problems*. IEEE Trans. on Magn. MAG-18, 284-292, 1982.
[25] Clavel E., Roudet J. and Foggia A.: *Electrical modeling of transformer connecting bars*. IEEE Trans. on Magn., Vol. 38, No. 2, 1378-1382, 2002.
[26] Paul C. R.: *Inductance: loop and partial.* J Wiley & Sons, New Jersey, 2010.
[27] Zhihua Z. and Weiming M.: *AC impedance of an isolated flat conductor*. IEEE Trans. on Electromagnetic Compatibility, Vol. 44, No. 3, 2002, pp. 482-486.
[28] Baron B. et al: *Impedance of an isolated rectangular conductor*. Przegląd Elektrotechniczny (Electrical Review), 2013 (to be published).
[29] Matsuki M. and Matsushima A.: *Improved numerical method for computing internal impedance of a rectangular conductor and discussions of its high frequency behavior*. Progress in Electromagnetics Research M, Vol. 23, 139-152, 2012.
[30] Matsuki M. and Matsushima A.: *Efficient impedance computation for multiconductor transmission lines of rectangular cross section*. Progress in Electromagnetics Research B, Vol. 43, 373-391, 2012.

Authors: *Prof. dr hab. inż. Zygmunt Piątek, Pol. Częstochowska, Instytut Inżynierii Środowiska, e-mail: zygmunt.piatek@interia.pl*
Prof. dr hab. inż. Bernard Baron, Pol. Śląska, Instytut Elektrotechniki i Informatyki, e-mail: bernard.baron@polsl.pl
Dr inż. Paweł Jabłoński, Pol. Częstochowska, Instytut Elektrotechniki Przemysłowej, e-mail: paweljablonski7@gmail.com
Dr inż. Tomasz Szczegielniak, Pol. Częstochowska, Instytut Inżynierii Środowiska, e-mail: szczegielniakt@interia.pl
Dr inż. Dariusz Kusiak, Pol. Częstochowska, Instytut Elektrotechniki Przemysłowej, e-mail: dariuszkusiak@wp.pl
Dr inż. Artur Pasierbek, Pol. Śląska, Instytut Elektrotechniki i Informatyki, e-mail: artur.pasierbek@polsl.pl